Micro-Shape Control, Riblets and Drag Minimization

Matthieu Bonnivard, Dorin Bucur

Micro shape control, riblets and drag minimization

Matthieu Bonnivard Dorin Bucur

Laboratoire de Mathématiques, CNRS UMR 5127, Université de Savoie
Campus Scientifique, 73376 Le-Bourget-Du-Lac, France

Abstract

Relying on the rugosity effect, we analyse the drag minimization problem in relation with the micro-structure of the surface of a given obstacle. We construct a mathematical framework for the optimisation problem, prove the existence of an optimal solution by Γ-convergence arguments and analyse the stability of the drag with respect to the micro-structure. Within our mathematical model, we explain why riblets may decrease the drag and also discuss complex rugosity effects related to synthetic jets or dynamic rugosity, modeled by combinations of rugous regions with in-flow and out-flow micro-perforations. Finally, numerical computations are performed in order to support the theoretical results.

Keywords: drag minimization, rugosity effect, micro-shape control

1 Introduction

The main purpose of the paper is to analyse the drag minimization problem in relation with the micro-structure on the surface of a shape. The minimization of the drag with respect to the shape is a debated question. Given a model for the fluid motion and a contact law (e.g. stationary Navier Stokes equations with total adherence conditions), the question of optimizing the shape in order to minimize the drag may be answered in the classical framework of shape optimization problems (see [11], [12], [9], [8], [13], [6]). In this paper, the drag minimization problem is attacked from a different point of view. Our problem is the following: given a fixed shape S and a non perfectly adherent material, the purpose is to create a microscopic structure on the surface of the shape such that the drag diminishes. We set the problem in terms of the rugosity effect relying on the friction-driven boundary conditions [3] and prove the existence of a solution which, loosely speaking, may be approached by a family of riblets with rough bottoms.

It is commonly accepted that rough surfaces *increase* the drag. From a mathematical point of view this is true as soon as one deals with fluids obeying to Stokes equations (see Section 3). In the context of Navier-Stokes flows, it was noticed that contrary to this reasonable observation, the drag may decrease in contact with rough surfaces (e.g. the shark's skin). In this paper, we intend to give a mathematical formulation to this micro-shape

optimization problem, to analyse the question of the existence of an optimal micro-structure and to provide some numerical computations supporting our observations.

A fundamental (mathematical) observation is the following: creating a micro-structure (riblets, denticles, etc.) on perfectly adherent material will produce an insignificant variation of the drag, since the variations of the solution to the Navier-Stokes equations are small. Experimental observations of this mathematical result are listed in [14]. On the contrary, a micro-structure on a slippery material may significantly change the solution to the Navier-Stokes equations. And surprisingly, adding rugosity may diminish the drag! This is true, provided that the drag function is not increasing with respect to the "amount of rugosity" (see the precise sense in Section 3). We observe numerically that this is the case for Navier-Stokes flows, and prove rigorously that this behaviour cannot be observed for Stokes flows.

We set the problem as follows. We assume that the shape of the obstacle is fixed and that the material is not perfectly adherent (for simplicity, we consider a perfectly slippery material). We define the control space as the family of friction-driven boundary conditions (in the sequel called *micro-structures*, see [3]) resulting from the asymptotic behaviour of the rugosities on the surface of the material. We study the influence of the micro-structure on the drag and analyse the drag optimization problem with respect to the micro-structure for both Stokes and stationary Navier-Stokes equations. We prove that for Stokes equations, the drag satisfies a certain monotonicity property with respect to the micro-structure, so that riblets cannot be used to diminish the drag of an obstacle in a Stokes flow. On the contrary, for Navier-Stokes equations, this is not the case anymore. Of course, one can reasonably expect the drag to be lower, in general, for perfect slip boundary conditions than for perfect adherence, even for Navier-Stokes flows. Nevertheless, since perfect materials do not exist, the true question is the following: considering a certain material with a given friction law, can we diminish the drag by fashioning a suitable rugosity on the surface? As we notice that there is no monotonicity property (see Section 5 for numerical evidence), decreasing the drag by introducing rugosity is generally a possible issue.

Although we are not able to give a full answer to the optimization problem, the main objectives of the paper are:

- to introduce a mathematical framework for the drag optimization problem with respect to the micro-structure of the surface. For this purpose, we develop a Γ-convergence framework and study the drag as a function of the micro-structure;
- to prove that for Navier-Stokes equations the problem is well-posed and admits a solution in terms of friction-driven boundary conditions;
- to show that for Stokes equations, the drag can not be minimized as a consequence of the rugosity effect;
- to give an example of complex rugosity effect related to dynamic rugosity and synthetic jets, modeled by combinations of perfectly slippery regions with in-flow and out-flow micro perforations;
- to perform numerical computations to support the mathematical results. Our computations justify the optimization approach and confirm the non-monotonicity of the drag with respect to the friction-driven boundary conditions for Navier-Stokes equations.

The structure of the paper is the following. In Section 2, we introduce the mathematical approach of the rugosity effect and recall the main results of [3]. In Section 3, we develop the mathematical framework for the drag minimization, prove the existence of a solution and discuss the monotonicity of the drag with respect to the friction-driven boundary conditions. Section 4 is devoted to the complex rugosity effect related to dynamic rugosity and synthetic jets, which falls out of the friction-driven boundary conditions obtained in [3] and naturally enlarge the space of controls. In Section 5, we perform numerical computations to support the non-monotonicity argument and give some examples.

2 The rugosity effect: a mathematical background

Capacitary measures. Let $D \subseteq \mathbb{R}^N$ be a bounded open set. The capacity of a subset E in D is

$$\mathrm{cap}(E, D) = \inf\Big\{ \int_D |\nabla u|^2 \, \mathrm{d}x \ : u \in \mathcal{U}_E \Big\},$$

where $\mathcal{U}_E$ is the set of all functions u of the Sobolev space $H^1_0(D)$ such that $u \geq 1$ almost everywhere in a neighborhood of E.

If a property $P(x)$ holds for all $x \in E$ except for the elements of a set $Z \subseteq E$ with $\mathrm{cap}(Z) = 0$, we say that $P(x)$ holds *quasi-everywhere* on E (shortly *q.e.* on E). The expression *almost everywhere* (shortly *a.e.*) refers, as usual, to the Lebesgue measure. A subset A of D is said to be *quasi-open* if for every $\varepsilon > 0$ there exists an open subset A_ε of D, such that $A \subseteq A_\varepsilon$ and $\mathrm{cap}(A_\varepsilon \setminus A, D) < \varepsilon$. A function $f \colon D \to \mathbb{R}$ is said to be *quasi-continuous* if for every $\varepsilon > 0$ there exists a continuous function $f_\varepsilon \colon D \to \mathbb{R}$ such that $\mathrm{cap}(\{f \neq f_\varepsilon\}, D) < \varepsilon$, where $\{f \neq f_\varepsilon\} = \{x \in D : f(x) \neq f_\varepsilon(x)\}$. It is well known (see, e.g., Ziemer [15]) that every function u of the Sobolev space $H^1(D)$ has a quasi-continuous representative, which is uniquely defined up to a set of capacity zero. We shall always identify the function u with its quasi-continuous representative, so that a pointwise condition can be imposed on $u(x)$ for quasi-every $x \in D$.

We note $\mathcal{M}_0(D)$ the set of all nonnegative Borel measures μ on D, possibly $+\infty$ valued, such that

i) $\mu(B) = 0$ for every Borel set $B \subseteq D$ with $\mathrm{cap}(B, D) = 0$,

ii) $\mu(B) = \inf\{\mu(U) : U \text{ quasi-open}, \ B \subseteq U\}$ for every Borel set $B \subseteq D$.

We stress the fact that the measures $\mu \in \mathcal{M}_0(D)$ do not need to be finite, and may take the value $+\infty$ even on large parts of D.

Given an arbitrary subset E of D, we note $\infty|_E$ the measure defined by

i) $\infty|_E(B) = 0$ for every Borel set $B \subseteq D$ with $\mathrm{cap}(B \cap E, D) = 0$,

ii) $\infty|_E(B) = +\infty$ for every Borel set $B \subseteq D$ with $\mathrm{cap}(B \cap E, D) > 0$.

For a quasi-open set A, we always identify A with the measure $\infty_{D\setminus A}$ and observe that $H^1_0(D) \cap L^2(D, \infty_{D\setminus A}) = H^1_0(A)$ (see [7, 2]).

Navier-Stokes equations with friction-driven boundary conditions in $\mathbb{R}^3$. Let S be a closed Lipschitz subset of a smooth bounded open set $\Omega \subseteq \mathbb{R}^3$. Let $\mu \in \mathcal{M}_0(D)$ be concentrated on ∂S. We consider a family of linear spaces $\mathcal{V} := \{V(x)\}_{x\in\partial S}$, where $V(x)$ is a subspace of the tangent hyperplane (where it exists) at $x \in \partial S$. In particular, the dimension of $V(x)$ does not exceed 2. Furthermore, let $a_{i,j} : \partial S \to \mathbb{R}$, $1 \le i, j \le 3$, be Borel functions such that $a_{i,j} = a_{j,i}$, and $\sum_{i,j=1}^3 a_{ij}\xi_i\xi_j \ge 0$ for all $\xi \in \mathbb{R}^3$. We set $A = \{a_{i,j}\}_{i,j=1}^3$.

Following [3], Navier-Stokes problem with friction-driven boundary conditions reads: find $(\mathbf{u}, p) \in \mathbf{H}^1(\Omega \setminus S) \times L^2_0(\Omega \setminus S)$ such that

$$-\text{div } \sigma(\mathbf{u}, p) + (\mathbf{u} \cdot \nabla)\mathbf{u} = 0 \text{ in } \Omega \setminus S, \tag{1}$$

$$\text{div } \mathbf{u} = 0 \text{ in } \Omega \setminus S, \tag{2}$$

$$\mathbf{u} = \mathbf{u}_\infty \text{ on } \partial\Omega, \tag{3}$$

$$\mathbf{u}(x) \in V(x) \text{ for q.e. } x \in \partial S, \tag{4}$$

$$\Big[2\nu\mathbf{D}(\mathbf{u})\mathbf{n} + \mu A\mathbf{u}\Big] \cdot \mathbf{v} = 0 \text{ for } \mathbf{v} \in V(x),\ x \in \partial S, \tag{5}$$

where $\sigma(\mathbf{u}, p)$ is the stress tensor defined by

$$\sigma(\mathbf{u}, p) = 2\nu\mathbf{D}(\mathbf{u}) - p\text{Id},$$

$\mathbf{D}(\mathbf{u})$ being the symmetric part of $\nabla\mathbf{u}$ defined by

$$\mathbf{D}(\mathbf{u}) = \frac{1}{2}\left((\nabla\mathbf{u}) + (\nabla\mathbf{u})^T\right).$$

Above, $\Big[2\nu\mathbf{D}(\mathbf{u}) \cdot \mathbf{n} + \mu A\mathbf{u}\Big] \cdot \mathbf{v} = 0$ for $\mathbf{v} \in V(x)$, is a formal pointwise relation, which has to be understood globally on ∂S. Precisely, condition (5) holds provided that

$$2\nu \int_{\partial S} \mathbf{D}(\mathbf{u})\mathbf{n} \cdot \mathbf{v}\mathrm{d}x + \int_{\partial S} A\mathbf{v} \cdot \mathbf{v}\mathrm{d}\mu = 0$$

for every $\mathbf{v} \in \mathbf{H}^1(\Omega \setminus S)$ such that $\mathbf{v}(x) \in V(x)$ for q.e. $x \in \partial S$.

We say that $(\mathbf{u}, p) \in \mathbf{H}^1(\Omega \setminus S) \times L^2_0(\Omega \setminus S)$ is a weak solution to System (1)-(5) provided that $\mathbf{u} \in H^1(\Omega \setminus S, \mathbb{R}^3)$ is such that div $\mathbf{u} = 0$ in $\Omega \setminus S$, $\mathbf{u}(x) \in V(x)$ for q.e. $x \in \partial S$, $\mathbf{u}(x) = \mathbf{u}_\infty(x)$ on $\partial\Omega$, and satisfies

$$2\nu \int_{\Omega\setminus S} \mathbf{D}(\mathbf{u}) : \mathbf{D}(\phi)\ \mathrm{d}x + \int_{\Omega\setminus S} [(\mathbf{u} \cdot \nabla)\mathbf{u}] \cdot \phi\ \mathrm{d}x + \int_{\partial S} A\mathbf{u} \cdot \phi\ d\mu = 0, \tag{6}$$

for every $\phi \in \mathbf{H}^1(\Omega \setminus S)$ such that div $\phi = 0$ in $\Omega \setminus S$, $\phi(x) \in V(x)$ for q.e. $x \in \partial S$ and $\phi(x) = 0$ on $\partial\Omega$. Above, $\mathbf{u}_\infty$ can be considered as an arbitrary function in $\mathbf{H}^{1/2}(\partial\Omega)$ with zero mean value on $\partial\Omega$, but for our purposes, $\mathbf{u}_\infty$ is a constant vector fields representing the velocity of the fluid at infinity.

Notice that if $A \equiv 0$, $\mu \equiv 0$ and for q.e. $x \in \partial S, V(x) = \mathbb{R}^2$, then the friction-driven boundary conditions are precisely the perfect slip ones. If $A = \text{Id}$ and $\mu = +\infty\lfloor_{\partial S}$, or if for q.e. $x \in \partial S$, $V(x) = \{0\}$, then the boundary conditions correspond to complete adherence.

The rugosity effect. We consider a sequence S_ε of equi-Lipschitz closed sets, converging to S in the Hausdorff metric (see the precise definition in the next section). The main result of [3] reads as follows.

Theorem 2.1 *Let $\varepsilon \to 0$ and $\{\mathbf{u}_\varepsilon\}_{\varepsilon>0}$ be a family of (weak) solutions to Navier-Stokes equations* (1)-(5) *in $\Omega \setminus S_\varepsilon$ with perfect slip conditions on ∂S_ε, with uniformly bounded energies, i.e. $\exists M > 0, \forall \varepsilon > 0, \|\mathbf{u}_\varepsilon\|_{\mathbf{H}^1(\Omega\setminus S_\varepsilon)} \leq M$.*

Then, at least for a suitable subsequence,

$$1_{\Omega\setminus S_\varepsilon}\mathbf{u}_\varepsilon \to 1_{\Omega\setminus S}\mathbf{u} \text{ (strongly) in } L^2(\mathbb{R}^3,\mathbb{R}^3),$$

$$1_{\Omega\setminus S_\varepsilon}\nabla\mathbf{u}_\varepsilon \to 1_{\Omega\setminus S}\nabla\mathbf{u} \text{ weakly in } L^2(\mathbb{R}^3,\mathbb{R}^{3\times 3}),$$

and there exists a suitable triplet $\{\mu, A, \mathcal{V}\}$ independent on $\mathbf{u}_\infty$ such that

- *μ is a capacitary measure concentrated on ∂S,*
- *$\mathcal{V} = \{V(x)\}_{x\in\Gamma}$ is a family of vector subspaces in $\mathbb{R}^2$,*
- *A is a positive symmetric matrix function defined on ∂S,*

and $\mathbf{u}$ is a solution in $\Omega \setminus S$ to Navier-Stokes equations with friction-driven boundary conditions (1)-(5).

We underline that the triplet $\{\mu, A, \mathcal{V}\}$ is of geometric nature, being independent on $\mathbf{u}_\infty \in \mathbf{H}^{1/2}(\partial\Omega)$. By abuse of language, we call *micro-structure* a triplet $\{\mu, A, \mathcal{V}\}$.

3 Drag optimization with respect to the micro-structure

In a first step, we introduce the family of admissible micro-structures. A micro-structure $\{\mu, A, \mathcal{V}\}$ is admissible as soon as it is obtained through the rugosity effect, i.e. is a limit obtained from a sequence $(S_\varepsilon)_{\varepsilon>0}$ in the frame of Theorem 2.1. For technical purposes, the family of rugous sets $S_\varepsilon \subseteq \Omega$ is assumed to have a uniform Lipschitz character, precisely to satisfy the uniform cone condition (see [8, Definition 2.4.1]). More specifically, given $\pi/2 > \omega > 0$, $h > 0$, let

$$C(x,\omega,h,\xi) = \{y \in \mathbb{R}^N : \|y-x\| \leq h, (y-x,\xi) > \cos(\omega)\|y-x\|\}$$

be the cone with vertex at x, operture 2ω, height h, and orientation given by a unit vector ξ. The uniform cone condition requires the existence of fixed $\omega > 0$ and $h > 0$ such that for any $\varepsilon > 0$, $x_0 \in \partial S_\varepsilon$, there exists a unit vector $\xi_{x_0} \in \mathbb{R}^N$ such that

$$C(x,\omega,h,\xi_{x_0}) \subseteq \Omega \setminus S_\varepsilon \text{ whenever } x \in B(x_0,\omega) \cap \overline{\Omega \setminus S_\varepsilon}.$$

In addition, we assume that the family $\{S_\varepsilon\}_{\varepsilon>0}$ converges to S in the sense that

$$1_{S_\varepsilon} \to 1_S \text{ in } L^1(\Omega) \text{ as } \varepsilon \to 0 \tag{7}$$

where 1_S is the characteristic function of S. As a direct consequence of the uniform cone condition, the sequence of domains converges also in the Hausdorff topology, specifically,

$$d(\cdot, S_\varepsilon) \to d(\cdot, S) \text{ uniformly on } \Omega, \tag{8}$$

where $d(\cdot, F)$ denotes the distance function to the set F.

Definition 3.1 *Let $\{\mu_\varepsilon, A_\varepsilon, \mathcal{V}_\varepsilon\}$ be defined on ∂S_ε. We say that $\{\mu_\varepsilon, A_\varepsilon, \mathcal{V}_\varepsilon, S_\varepsilon\}$ γ-converges to $\{\mu, A, \mathcal{V}, S\}$ if S_ε and S satisfy (7)-(8) and the functionals*

$$F_\varepsilon(\mathbf{v}) = \begin{cases} 2\nu \displaystyle\int_{\Omega\setminus S_\varepsilon} |\mathbf{D}(\mathbf{v})|^2 \mathrm{d}x + \int_{\partial S_\varepsilon} A_\varepsilon \mathbf{v}\cdot\mathbf{v}\mathrm{d}\mu_\varepsilon & \text{if } \mathbf{v}\in H_0^1(\Omega,\mathbb{R}^3),\ \text{div } \mathbf{v}=0 \text{ in } \Omega\setminus S_\varepsilon, \\ & \mathbf{v}(x)\in V_\varepsilon(x), \text{q.e. } x\in\partial S_\varepsilon, \\ +\infty & \text{otherwise,} \end{cases} \tag{9}$$

Γ-converges to F in $L^2(\Omega,\mathbb{R}^3)$, where

$$F(\mathbf{v}) = \begin{cases} 2\nu \displaystyle\int_{\Omega\setminus S} |\mathbf{D}(\mathbf{v})|^2 \mathrm{d}x + \int_{\partial S} A\mathbf{v}\cdot\mathbf{v}\mathrm{d}\mu & \text{if } \mathbf{v}\in H_0^1(\Omega,\mathbb{R}^3),\ \text{div } \mathbf{v}=0 \text{ in } \Omega\setminus S, \\ & \mathbf{v}(x)\in V(x), \text{q.e. } x\in\partial S, \\ +\infty & \text{otherwise.} \end{cases} \tag{10}$$

For the definition and properties of Γ-convergence, we refer the reader to [5].

Remark 3.2 Let us notice that the γ-convergence defined above implies the continuity of the solutions to Stokes equations with respect to the micro-structure. Indeed, let us consider Stokes equations in $\Omega\setminus S_\varepsilon$ with friction-driven boundary conditions $\{\mu_\varepsilon, A_\varepsilon, \mathcal{V}_\varepsilon\}$, i.e.

$$-\text{div } \sigma(\mathbf{u},p) = 0 \text{ in } \Omega\setminus S, \tag{11}$$

$$\text{div } \mathbf{u} = 0 \text{ in } \Omega\setminus S, \tag{12}$$

$$\mathbf{u} = \mathbf{u}_\infty \text{ on } \partial\Omega, \tag{13}$$

$$\mathbf{u}(x)\in V(x) \text{ for q.e. } x\in\partial S, \tag{14}$$

$$\Big[2\nu\mathbf{D}(\mathbf{u})\mathbf{n} + \mu A\mathbf{u}\Big]\cdot\mathbf{v} = 0 \text{ for } \mathbf{v}\in V(x),\ x\in\partial S. \tag{15}$$

The weak solution $\mathbf{u}_\varepsilon$ of Equations (11)-(15) is also the unique minimizer of

$$H_\varepsilon(\mathbf{v}) := 2\nu\int_{\Omega\setminus S_\varepsilon} |\mathbf{D}(\mathbf{v})|^2\mathrm{d}x + \int_{\partial S_\varepsilon} A_\varepsilon\mathbf{v}\cdot\mathbf{v}\mathrm{d}\mu_\varepsilon, \tag{16}$$

over

$$\mathcal{C}_\varepsilon := \Big\{\mathbf{v}\in H^1(\Omega,\mathbb{R}^3)\ \Big|\ \text{div } \mathbf{v}=0 \text{ in } \Omega,\ \mathbf{v}(x)\in V_\varepsilon(x) \text{ for q.e. } x\in\partial S_\varepsilon, \mathbf{v}=\mathbf{u}_\infty \text{ on } \partial\Omega\Big\}.$$

As $\mathcal{C}_\varepsilon$ is a closed subspace of $H^1(D\setminus S,\mathbb{R}^3)$, the classical Lax-Milgram theorem together with Korn's inequality give existence and uniqueness of the solution.

Let us note $\mathbf{u}_\infty\in H^1(\Omega,\mathbb{R}^3)$ an extension of $\mathbf{u}_\infty\lfloor_{\partial\Omega}$ which is vanishing on a neighborhood of S, and notice that for every $\mathbf{v}\in H^1(\Omega,\mathbb{R}^3)$ such that $\mathbf{v}=\mathbf{u}_\infty$ on $\partial\Omega$,

$$H_\varepsilon(\mathbf{v}) = F_\varepsilon(\mathbf{v}-\mathbf{u}_\infty) - 4\nu\int_{\Omega\setminus S_\varepsilon}\mathbf{D}(\mathbf{v}):\mathbf{D}(\mathbf{u}_\infty)\mathrm{d}x + 2\nu\int_{\Omega\setminus S_\varepsilon}|\mathbf{D}(\mathbf{u}_\infty)|^2\mathrm{d}x.$$

Consequently, H_ε Γ-converges in $L^2(\Omega,\mathbb{R}^3)$ to H, thus their minimizers converge also in $L^2(\Omega,\mathbb{R}^3)$. This is an immediate consequence of the fact that the minimizers are uniformly bounded in $H^1(\Omega,\mathbb{R}^3)$. The minimizer of H_ε is precisely the solution to Stokes equations (11)-(15).

Remark 3.3 In the language of γ-convergence, Theorem 2.1 asserts that $\{0,0,\mathbb{R}^2,S_\varepsilon\} \xrightarrow{\gamma} \{\mu,A,\mathcal{V},S\}$. In fact, the proof of Theorem 2.1 is based on the Γ-convergence of the energy functionals, and on the fact that a continuous perturbation of a Γ-convergent sequence still Γ-converges, so that the conclusion of Theorem 2.1 remains valid if $\{\mu_\varepsilon,A_\varepsilon,\mathcal{V}_\varepsilon,S_\varepsilon\}$ γ-converges to $\{\mu,A,\mathcal{V},S\}$ (see Theorem 3.7 below). We emphasize that the geometric effect of the rugosity (i.e. the γ-limit) is the same on both Stokes and Navier-Stokes equations.

Remark 3.4 The topology of the γ-convergence is metrizable. This is a consequence of the uniform coerciveness of the functionals F_ε (see [5]). Indeed, we can formally change the functionals to make them equi-coercive by setting the value of F to $+\infty$ as soon as the L^2-norm of u on S_ε is not equi-dominated by $\int_{\Omega\setminus S_\varepsilon}|\mathbf{D}(\mathbf{u})|^2\mathrm{d}x$, i.e.

$$\|\mathbf{u}\|^2_{L^2(S_\varepsilon,\mathbb{R}^3)} \geq C\int_{\Omega\setminus S_\varepsilon}|\mathbf{D}(\mathbf{u})|^2\mathrm{d}x,$$

where C is suitably chosen, in relation with the constant bounding uniformly the norms of the extension operators from $H^1(\Omega\setminus S_\varepsilon)$ to $H^1(\Omega)$.

Remark 3.5 For a given obstacle S, the family of admissible micro-structures on the surface of S is

$$\mathcal{U} = \Big\{\{\mu,A,\mathcal{V},S\} : \exists S_\varepsilon \text{ such that } \{0,0,\mathbb{R}^2,S_\varepsilon\} \xrightarrow{\gamma} \{\mu,A,\mathcal{V},S\}\Big\}.$$

Perfectly slippery materials do not exist, so in practice one should restrict the class of admissible controls to the γ-limits of rugous domains satisfying a friction law given by a nonnegative friction coefficient β, precisely,

$$\mathcal{U}_\beta = \Big\{\{\mu,A,\mathcal{V},S\} : \exists S_\varepsilon \text{ such that } \{Id,\beta\mathrm{d}x,\mathbb{R}^2,S_\varepsilon\} \xrightarrow{\gamma} \{\mu,A,\mathcal{V},S\}\Big\}.$$

Theorem 3.6 *The families $\mathcal{U}$ and $\mathcal{U}_\beta$, endowed with the topology of the γ-convergence, are compact.*

Proof. Since the γ-convergence is metrisable, it is enough to prove sequential compactness. Let $\{\mu_n,A_n,\mathcal{V}_n,S\}$ be a sequence of micro-structures in $\mathcal{U}$ (the proof for $\mathcal{U}_\beta$ is similar). From the definition of the admissible micro-structures, for every $n\in\mathbb{N}$, there exists S_n such that

$$d_\gamma(\{0,0,\mathbb{R}^2,S_n\},\{\mu_n,A_n,\mathcal{V}_n,S\}) + d_H(S_n,S) \leq \frac{1}{n}.$$

We apply the result of Theorem 2.1 (see also Remark 3.3), so that, for a subsequence, there exists a triplet $\{\mu,A,\mathcal{V},S\}$ such that

$$\{0,0,\mathbb{R}^2,S_{n_k}\} \xrightarrow{\gamma} \{\mu,A,\mathcal{V},S\}.$$

Finally,

$$d_\gamma(\{\mu_{n_k}, A_{n_k}, \mathcal{V}_{n_k}, S\}, \{\mu, A, \mathcal{V}, S\}) \to 0.$$

□

Theorem 3.7 *The drag is γ-continuous for both Stokes and Navier-Stokes equations.*

Proof. For Stokes equations, the expression of the drag reads

$$T(\{\mu_n, A_n, \mathcal{V}_n, S_n\}) = -\int_{\partial S_n} \sigma(\mathbf{u}_n, p_n)\mathbf{n} \cdot \mathbf{u}_\infty \mathrm{d}s,$$

which turns out to be twice the energy of Stokes system

$$\nu \int_{\Omega \setminus S_n} |\mathbf{D}(\mathbf{u}_n)|^2 \, \mathrm{d}x + \frac{1}{2} \int_{\partial S_n} A_\varepsilon \mathbf{u}_n \cdot \mathbf{u}_n \mathrm{d}\mu_n,$$

$\mathbf{u}_n$ being the solution to Stokes equations. Following Remark 3.2, in the case of Stokes equations, Theorem 3.7 is a direct consequence of the convergence of minima in the general framework of Γ-convergence.

Since the solution to Navier-Stokes equations may not be unique, the assertion of Theorem 3.7 has to be understood as follows. Assume that

$$\{\mu_n, A_n, \mathcal{V}_n, S_n\} \xrightarrow{\gamma} \{\mu, A, \mathcal{V}, S\},$$

and let $(\mathbf{u}_n)_{n\in\mathbb{N}}$ be a family of weak solutions to Navier-Stokes equations with friction-driven boundary conditions $\{\mu_n, A_n, \mathcal{V}_n\}$ on S_n. For every $n \in \mathbb{N}$, we note $T(\{\mu_n, A_n, \mathcal{V}_n, S_n\}, \mathbf{u}_n)$ the corresponding drag. If $\sup_n T(\{\mu_n, A_n, \mathcal{V}_n, S_n\}) < +\infty$, there exists a subsequence and a solution $\mathbf{u}$ to the limit Navier-Stokes equations, such that

$$T(\{\mu_{n_k}, A_{n_k}, \mathcal{V}_{n_k}, S_{n_k}\}, \mathbf{u}_k) \to T(\{\mu, A, \mathcal{V}, S\}, \mathbf{u}).$$

Indeed, since $\sup_n T(\{\mu_n, A_n, \mathcal{V}_n, S_n\}, \mathbf{u}_n) < +\infty$, we can assume that $\sup_n \|\mathbf{u}_n\|_{H^1(\Omega,\mathbb{R}^3)} < +\infty$, and consequently, that there exists a subsequence (still noted with the same index) such that $\mathbf{u}_n \rightharpoonup \mathbf{u}$ weakly in $H^1(\Omega, \mathbb{R}^3)$. In particular,

$$1_{\Omega\setminus S_n}\mathbf{u}_n \to 1_{\Omega\setminus S}\mathbf{u} \text{ (strongly) in } L^2(\mathbb{R}^3, \mathbb{R}^3),$$

$$1_{\Omega\setminus S_n}\nabla\mathbf{u}_n \to 1_{\Omega\setminus S}\nabla\mathbf{u} \text{ weakly in } L^2(\mathbb{R}^3, \mathbb{R}^{3\times 3}).$$

We define $f_n = -1_{\Omega\setminus S_n}(\mathbf{u}_n \cdot \nabla)\mathbf{u}_n \in H^{-1}(\Omega, \mathbb{R}^3)$, and notice that $f_n \to f := -1_{\Omega\setminus S}\mathbf{u} \cdot \nabla\mathbf{u}$ strongly in $H^{-1}(\Omega, \mathbb{R}^3)$.

Since $H_n \xrightarrow{\Gamma} H$, we observe that

$$\frac{1}{2}F_n(\cdot) - < f_n, \cdot >_{H^{-1}(\Omega)\times H^1_0(\Omega)} \xrightarrow{\Gamma} \frac{1}{2}F(\cdot) - < f, \cdot >_{H^{-1}(\Omega)\times H^1_0(\Omega)} .$$

Since $\mathbf{u}_n$ are minimizers of the modified functionals and they converge to $\mathbf{u}$, we get that $\mathbf{u}$ is a minimizer of $\frac{1}{2}H(\cdot) - < f, \cdot >_{H^{-1}(\Omega)\times H^1_0(\Omega)}$. As a result, $\mathbf{u}$ is a solution to Navier-Stokes equations, since it satisfies the Euler equation associated to a minimizer.

Taking $\mathbf{u}_n - \mathbf{u}_\infty$ and $\mathbf{u} - \mathbf{u}_\infty$ as test functions in the respective weak formulations, we get that

$$T(\{\mu_n, A_n, \mathcal{V}_n, S_n\}, \mathbf{u}_n) =$$
$$2\nu \int_{\Omega \setminus S_n} \mathbf{D}(\mathbf{u}_n) : \mathbf{D}(\mathbf{u}_\infty) \mathrm{d}x + \int_{\partial S_n} A_n \mathbf{u}_n \cdot \mathbf{u}_\infty \mathrm{d}\mu + < f_n, \mathbf{u}_n - \mathbf{u}_\infty >_{H^{-1}(\Omega) \times H_0^1(\Omega)} .$$

The right hand side passes to the limit since $\mathbf{u}_n$ converges weakly in $H^1(\Omega, \mathbb{R}^3)$, the boundary term $\int_{\partial S_n} A_n \mathbf{u}_n \cdot \mathbf{u}_\infty \mathrm{d}\mu$ vanishes and $f_n \to f$ strongly in $H^{-1}(\Omega, \mathbb{R}^3)$. □

Theorem 3.7 provides two pieces of information. The first one is practical: the drag associated to friction-driven boundary conditions is close to the drag associated to rugous domains which γ-converge. Thus, optimal friction-driven boundary conditions can be approached by rugous domains. Second, from a mathematical point of view, if two micro-structures are close in the γ-distance, the associated drags are also close.

Corollary 3.8 *The drag minimization problem on $\mathcal{U}$, respectively $\mathcal{U}_\beta$, has at least one solution.*

Proof. This is a direct consequence of Theorems 3.6 and 3.7. □

Drag monotonicity for Stokes equations. We consider Stokes equations with friction-driven boundary conditions (11)-(15) associated to a fixed obstacle S and different micro-structures $\{\mu, A, \mathcal{V}\}$.

Theorem 3.9 *Assume that $\{\mu_1, A_1, \mathcal{V}_1\} \leq \{\mu_2, A_2, \mathcal{V}_2\}$ in the following sense:*

$$\forall \xi \in H^1(D \setminus S) \quad \int_{\partial S} A_1 \xi \cdot \xi \mathrm{d}\mu_1 \leq \int_{\partial S} A_2 \xi \cdot \xi \mathrm{d}\mu_2,$$
$$\textit{for q.e. } x \in \partial S,\ V_2(x) \subseteq V_1(x).$$

Then

$$T(\{\mu_1, A_1, \mathcal{V}_1, S\}) \leq T(\{\mu_2, A_2, \mathcal{V}_2, S\}).$$

Proof. The proof is a direct consequence of the energetic formulation of Stokes equations and the inclusion of the energy spaces. □

Remark 3.10 Since perfect slip boundary conditions correspond to

$$A_1 = 0, \mu_1 = 0, V_1(x) = \mathbb{R}^2,$$

and perfect adherence, to

$$A_2 = Id, \mu_2 = \infty \lfloor_{\partial S}, V_2(x) = \{0\},$$

the drag of an obstacle associated to perfect slip boundary conditions is lower than for perfect adherence.

Remark 3.11 Let us consider a riblet structure given by

$$A = 0, \mu = 0, V(x) = \xi(x) \cdot \mathbb{R},$$

where $\xi : \partial S \to S^1$. Clearly, the value of the drag associated to this structure is between the extremal ones. Nevertheless, the monotonicity is not strict since a good choice of the riblets ξ can give the optimal drag associated to the perfect slip conditions for a given $\mathbf{u}_\infty$.

4 Example of complex rugosity effect

Modelling a highly complex rough surface like the scales on a shark skin is out of the mathemaical purposes of the paper. Nevertheless, some features of this very singular surface can be loosely approached. Fine movements of the scales may drive a thin fluid layer through the free vertical spaces between the scales, so that from a mathematical point of view one should consider beside the "large" riblet surfaces of the scales, small vertical regions where the fluid flow can be oriented. This phenomenon is similar to synthetic jets, which consist in blowing and sucking fluid through thin holes on the surface, using electronic devices (see [10, Section 1.2.3]).

The purpose of this section is to give an example of such a phenomenon where a suitable geometric distribution of these vertical singularities produce the following effect on the flow:

- the flow is driven in the direction of the riblets, as expected in the frame of the friction-driven boundary conditions;
- moreover, an orientation of the flow (inside the riblets) is obtained over the full boundary as a consequence of the jets through the tiny holes, i.e. , not only is the direction imposed, but also the sense.

We treat this example only at an energetic level, formulated as a mathematical result describing the asymptotic behaviour of a sequence of Sobolev functions satisfying these mixed boundary conditions. Transporting this kind of result to understand the full behaviour of the solutions of Navier-Stokes equations should follow the same steps as in [3]. However, it exceeds the purposes of the paper.

From the point of view of the drag minimization question, the main conclusion of this example is that the orientation of the flow can be seen as a new type of rugosity effect, out of the class of friction-driven boundary conditions, which effectively increases the space of controls $\mathcal{U}_C$ introduced in Section 3, opening new perspectives for the drag minimization.

Let S_ε be closed subsets of Ω satisfying a uniform cone condition and which converge to S in the Hausdorff metric. We assume that he surfaces ∂S_ε are divided in three regions: a "large" slip region S_ε and two small regions O_ε and I_ε, corresponding to the out-flow and in-flow of synthetic jets, which consist of tiny holes (arbitrarily) distributed over ∂S_ε. As well, we consider a bounded sequence of functions $\mathbf{u}_\varepsilon \in H^1(\Omega, \mathbb{R}^3)$ satisfying $\int_{\partial S_\varepsilon} \mathbf{u}_\varepsilon \cdot \mathbf{n}_\varepsilon \mathrm{d}s = 0$, which converges weakly to $\mathbf{u}$ in H^1 and satisfy the following assumptions:

- $\mathbf{u}_\varepsilon \cdot \mathbf{n}_\varepsilon = \omega_\varepsilon$, on S_ϵ

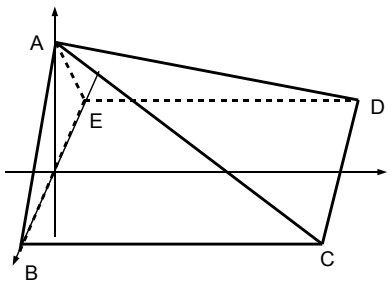

Figure 1: Shape of an elementary piece of rugosity.

- $\mathbf{u}_\varepsilon \cdot \mathbf{n}_\varepsilon \geq \alpha,$ on O_ϵ
- $\mathbf{u}_\varepsilon \cdot \mathbf{n}_\varepsilon \leq -\beta,$ on I_ϵ

The functions ω_ε above satisfy $\|\omega_\varepsilon\|_{L^\infty} \to 0$ and correspond to a possibly moving part of the perfect slip boundary, where the normal velocity is given by the movement of the shape. Depending on the distribution of the tiny holes, in the limit process, we may get the non-penetration condition $\mathbf{u} \cdot \mathbf{n} = 0$ on ∂S and, for example, to completely cancel the in-flow effect and completely enhance the out-flow effect by getting an orientation of the flow on the full surface of S. Precisely, one may expect the existence of a tangent field $\xi : \partial S \to S^2$, $\xi(x) \in T(x)$ depending only on the asymptotic behaviour of O_ε, such that $\mathbf{u}(x) \cdot \xi(x) \geq \alpha$ a.e. on ∂S.

We give a 3D example involving rugosities built from elementary pyramids similar to $ABCDE$, with $A(0,0,h)$, $B(0,\frac{l}{2},0)$, $C(L,\frac{l}{2},0)$, $D(L,-\frac{l}{2},0)$, $E(0,-\frac{l}{2},0)$ (see Figure 1). The rugosity we consider is given by an arbitrary union of pyramids similar to $ABCDE_i^\varepsilon$, with random sizes $(h_i^\varepsilon, l_i^\varepsilon, L_i^\varepsilon)$, which are flattening in the sense that $\max_\varepsilon \max_i h_i^\varepsilon \to 0$ for $\varepsilon \to 0$. For simplicity, we choose $O_\varepsilon = \emptyset$ and $\beta = 0$. As well, on the flattening faces $[ABC]_i^\varepsilon \cup [ACD]_i^\varepsilon \cup [ADE]_i^\varepsilon$ the normal component of the flow is a given by the function ω_ε while on the vertical face $[ABE]_i^\varepsilon$ the normal component of the flow is non positive.

Precisely, let

$$\sigma_\varepsilon = \{(x_i^\varepsilon, y_i^\varepsilon), i \in I_\varepsilon\} \subseteq [0,1]^2,$$

such that for every $i \in I_\varepsilon$, the rectangles

$$R_i^\varepsilon = (x_i^\varepsilon, x_i^\varepsilon + L_i^\varepsilon) \times (y_i^\varepsilon, y_i^\varepsilon + l_i^\varepsilon)$$

are disjoint and contained in $[0,1]^2$. We assume that $\alpha_1 \leq \frac{l_i^\varepsilon}{L_i^\varepsilon} \leq \alpha_2$ and define

$$\|\sigma_\varepsilon\| = \max_{i \in I_\varepsilon} L_i^\varepsilon + \left| [0,1]^2 \setminus \cup_{i \in I_\varepsilon} R_i^\varepsilon \right|.$$

Let $\varphi_\varepsilon : [0,1]^2 \to \mathbb{R}_+$ be an upper semicontinuous function defined by

$$\varphi_\varepsilon(x,y) = 0 \text{ for } x \in (0,1) \setminus \cup_{i \in I_\varepsilon} \overline{R}_i^\varepsilon, \qquad \varphi_\varepsilon = \max_i \tilde{\varphi}_\varepsilon^i \text{ for } x \in \cup_{i \in I_\varepsilon} \overline{R}_i^\varepsilon,$$

where $\tilde{\varphi}_\varepsilon^i\lfloor_{\overline{R}_i^\varepsilon}$ is the lowest concave function satisfying

$$\tilde{\varphi}_\varepsilon^i(x_i^\varepsilon+\delta_1 L_i^\varepsilon, y_i^\varepsilon+\delta_2 l_i^\varepsilon)=0; \delta_{1,2}\in\{0,1\}, \tilde{\varphi}_\varepsilon^i(x_i^\varepsilon+L_i^\varepsilon, y_i^\varepsilon+\frac{l_i^\varepsilon}{2})=C^\varepsilon L_i^\varepsilon.$$

We define the domains Ω_ε by

$$\Omega_\varepsilon=\{(x,y,z)|(x,y)\in(0,1)^2, \varphi_\varepsilon(x,y)<z<1\}.$$

We note $\mathbf{n}_\varepsilon$ the ouward normal to Ω_ε and we split the lower boundary of Ω_ε as follows:

- $S_\varepsilon=\partial\Omega_\varepsilon\cap\{(x,y,\varphi_\varepsilon(x,y))|(x,y)\in\cup_{i\in I_\varepsilon}R_i^\varepsilon\}$, the slip part of the boundary;
- $I_\varepsilon=\partial\Omega_\varepsilon\cap\{(x,y,z)|x=x_i+L_i^\varepsilon, y\in(y_i,y_i+l_i^\varepsilon), 0\le z\le\varphi_\varepsilon(x,y)\}$, the in-flow part of the boundary, and
- $F_\varepsilon=\partial\Omega_\varepsilon\cap\{z=0\}$, the residual flat part of the boundary.

Proposition 4.1 *Assume that $\|\sigma_\varepsilon\|\to 0$. There exist $C^\varepsilon\to 0$ such that for every sequence of functions $\mathbf{u}_\varepsilon\in H^1(\Omega,\mathbb{R}^3)$ satisfying*

$$\mathbf{u}_\varepsilon\rightharpoonup\mathbf{u}$$

$$\mathbf{u}_\varepsilon=0 \text{ on } \partial\Omega_\varepsilon\setminus(S_\varepsilon\cup I_\varepsilon\cup F_\varepsilon), \|\mathbf{u}_\varepsilon\cdot\mathbf{n}_\varepsilon\|_{L^\infty(S_\varepsilon)}\to 0, \mathbf{u}_\varepsilon\cdot\mathbf{n}_\varepsilon\ge 0 \text{ on } I_\varepsilon, \mathbf{u}_\varepsilon\cdot\mathbf{n}_\varepsilon=0 \text{ on } F_\varepsilon$$

then

$$\mathbf{u}\cdot e_3=0 \text{ on } (0,1)^2\times\{0\},\quad \mathbf{u}\cdot e_1\ge 0 \text{ on } (0,1)^2\times\{0\}.$$

Proof. First, we prove that for every $C^\varepsilon\to 0$, the non penetration condition $\mathbf{u}\cdot e_3=0$ on $(0,1)^2\times\{0\}$ is achieved. In a second step, a special choice for C^ε will insure the orientation of the flow, $\mathbf{u}\cdot e_2\ge 0$ on $(0,1)^2\times\{0\}$.

Indeed, assume that $C^\varepsilon\to 0$, thus $\|\mathbf{n}_\varepsilon-e_3\|_{L^\infty(S_\varepsilon)}\to 0$. We have for almost every $(x,y)\in(0,1)^2$

$$\mathbf{u}_\varepsilon(x,y,\varphi_\varepsilon(x,y))-\mathbf{u}_\varepsilon(x,y,0)=\int_0^{\varphi_\varepsilon(x,y)}\frac{\partial\mathbf{u}_\varepsilon}{\partial z}\partial z.$$

Multiplying by $\mathbf{n}_\varepsilon(x,y,\varphi_\varepsilon(x,y))$, we obtain

$$\mathbf{u}_\varepsilon(x,y,\varphi_\varepsilon(x,y))\cdot\mathbf{n}_\varepsilon(x,y,\varphi_\varepsilon(x,y))-\mathbf{u}_\varepsilon(x,y,0)\cdot\mathbf{n}_\varepsilon(x,y,\varphi_\varepsilon(x,y))=\mathbf{n}_\varepsilon(x,y,\varphi_\varepsilon(x,y))\cdot\int_0^{\varphi_\varepsilon(x,y)}\frac{\partial\mathbf{u}_\varepsilon}{\partial z}\mathrm{d}z,$$

which yields

$$|\mathbf{u}_\varepsilon(x,y,0)\cdot e_3|\le|\mathbf{u}_\varepsilon(x,y,\varepsilon_\varepsilon(x,y))\cdot\mathbf{n}_\varepsilon(x,y,\varphi_\varepsilon(x,y))|_\infty$$
$$+|\mathbf{u}_\varepsilon(x,y,0)|\|\mathbf{n}_\varepsilon-e_3\|_{L^\infty(S_\varepsilon)}+|\varphi_\varepsilon|_\infty\left(\int_0^{\varphi_\varepsilon(x,y)}\|\frac{\partial\mathbf{u}_\varepsilon}{\partial z}\|^2dz\right)^{1/2}.$$

Consequently,

$$\int_{(0,1)^2\times\{0\}} |\mathbf{u}_\varepsilon(x,y,0)\cdot e_3|^2 \mathrm{d}x\mathrm{d}y \leq 3|\mathbf{u}_\varepsilon(x,y,\varepsilon_\varepsilon(x,y))\cdot \mathbf{n}_\varepsilon(x,y,\varphi_\varepsilon(x,y))|_\infty^2$$
$$+ 3\|\mathbf{n}_\varepsilon - e_3\|^2_{L^\infty(S_\varepsilon)} \int_{(0,1^2)} |\mathbf{u}_\varepsilon(x,y,0)|^2 \mathrm{d}x\mathrm{d}y + 3|\varphi_\varepsilon|_\infty^2 \|\frac{\partial \mathbf{u}_\varepsilon}{\partial z}\|^2_{L^2(\Omega)}.$$

Letting $\varepsilon \to 0$, using the continuity of the trace $H^1(\Omega) \to L^2((0,1)^2 \times \{0\})$, the non penetration condition follows.

In order to prove that the orientation of the flow holds for a special choice of C^ε, we rely on the capacity density condition approach developed in [4] and on the metrizability of the γ convergence. Assume in a first step that $C^\varepsilon = C$ is a constant independent on ε. Consequently, the vertical faces I_ε satisfy a capacity density condition so that

$$\Omega \setminus I_\varepsilon(C) \xrightarrow{\gamma} \Omega \setminus [0,1]^2 \times \{0\},$$

in the sense of the γ-convergence. By a diagonal procedure, relying on the metrizability of the γ-convergence, we find a sequence $C^\varepsilon \to 0$ such that

$$\Omega \setminus I_\varepsilon(C_\varepsilon) \xrightarrow{\gamma} \Omega \setminus [0,1]^2 \times \{0\}.$$

As a direct consequence, if $\mathbf{u}_\varepsilon \cdot e_1 \geq 0$ on I_ε then $(\mathbf{u}_\varepsilon \cdot e_1)^- = 0$ on I_ε and $(\mathbf{u}\cdot e_1)^- = 0$ on $[0,1]^2 \times \{0\}$

□

Remark 4.2 If the region S_ε has a subregion O_ε where only the out-flow sense is prescribed $\mathbf{u}_\varepsilon \cdot \mathbf{n}_\varepsilon \leq 0$, without any control on the L^∞ norm of $\mathbf{u}_\varepsilon$ on O_ε, but such that $\mathrm{cap}(O_\varepsilon) \to 0$, the conclusion of the previous theorem remains true. In that case the out-flow effect is completely cancelled and the inflow effect is enforced on the full boundary.

5 Numerical computations

The purpose of this section is to give some numerical evidence of our theoretical results, in particular to numerically justify that adding suitable rugosity on the surface of an obstacle in a Navier-Stokes flow may lead to decrease the drag. In order to simplify the numerical computations, we fix the dimension of the space $N = 2$. In this case, the "driven" part of the friction-driven boundary conditions is trivial since the dimensions of the tangent spaces are 0 or 1, which can be simultaneously treated as a friction law, as follows.

We consider problem (1)-(5), where the boundary conditions (4)-(5) take the form

$$\mathbf{u}\cdot\mathbf{n} = 0 \text{ on } \partial S, \tag{17}$$
$$[2\nu \mathbf{D}(\mathbf{u})\mathbf{n}]_{tan} + \beta \mathbf{u} = 0 \text{ on } \partial S. \tag{18}$$

Above, β is a nonnegative Borel function, possibly infinite valued, corresponding to the distribution of the friction coefficient on the boundary of the solid. Notice that if $\beta \equiv$

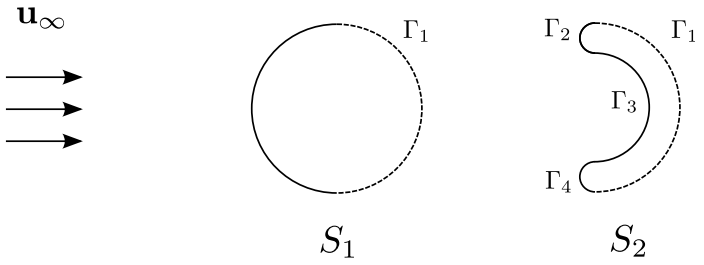

Figure 2: Two different shapes of the solid, a disk and an arch.

0, boundary conditions (17)-(18) correspond to perfect slip, and that perfect adherence is achieved formally by setting $\beta = +\infty$.

For every such β and every weak solution $(\mathbf{u}, p)$ to problem (1)–(3), (17)–(18), we denote $T(\beta, \mathbf{u})$ the corresponding drag, defined by

$$T(\beta, \mathbf{u}) = 2\nu \int_{\Omega \setminus S} |\mathbf{D}(\mathbf{u})|^2 \, \mathrm{d}x + \int_{\partial S} \beta |\mathbf{u}|^2 \mathrm{d}s.$$

In the numerical simulations, the domain Ω is the unit disk, $\mathbf{u}_\infty = (1, 0)$ and $\nu = 10^{-3}$. We consider two different shapes for the solid: a convex shape S_1, which is the disk of radius $R = 0.1$ centered at the origin, and a non convex shape S_2, which will be refered to as the *arch* in the remaining part of this section. The boundary of S_2 is composed by the union of four semicircles Γ_i with radius r_i, $i = 1...4$, defined by $r_1 = 0.1, r_2 = r_4 = 0.02$ and $r_3 = 0.06$ (see Figure 2). The center of Γ_1 coincides with the center of Ω.

The discretization is done by means of P_2 elements for the velocity and P_1 elements for the pressure, on a triangular mesh obtained by a Delaunay-Voronoi algorithm. In both configurations, 120 nodes are located on the boundary of Ω. In the S_1 configuration, the boundary of the solid is composed of 50 edges, and the mesh is composed of 9868 triangles. In the S_2 configuration, 80 nodes are located on the boundary of the arch, and we use 9476 elements. The stationnary Navier-Stokes equations is solved by a classic fix point iterative scheme. The incompressibility condition is treated by a Lagrange multiplier and the non penetration condition (17) is treated by penalisation.

Example 5.1 (Behaviour of the drag for constant friction coefficients.) In this example, we analyse the drag corresponding to values of the friction coefficient β which are assumed to be constant. The results are represented in Figure 3. We notice that in both cases, the drag is non decreasing with respect to *constant* functions β, which confirms the common intuition that, in general, the drag is higher for adherent materials than for slippery ones (even though this result is not mathematically proved for Navier-Stokes flows). More precisely, both curves have the aspect of a sigmoid: schematically, the drag is almost constant for $\beta \leq 0.001$, and then increases to reach its maximal value for $\beta \geq 1$.

Example 5.2 (Non monotonicity of the drag with respect to β.) In this example, we consider piecewise constant friction coefficients. We impose different constant values of the friction on Γ_1 and we fix $\beta = 10$ on the rest of the boundary. The results are represented

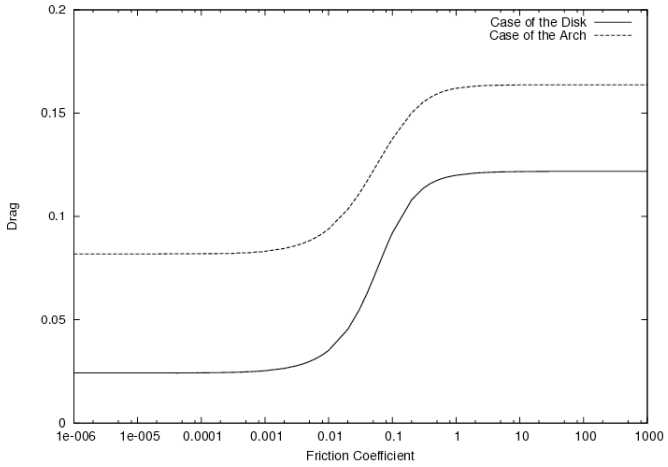

Figure 3: Drag values for constant friction coefficient.

in Figure 4. We notice that the drag is globally decreasing with respect to the value of β on $\partial S_1 \setminus \Gamma_1$ and $\partial S_2 \setminus \Gamma_1$. This behaviour is more significant in the case of the arch. In the latter case, the value of the drag for $\beta = 10$ on $\partial S_2 \setminus \Gamma_1$ is 3.23% inferior to its value for $\beta = 0.001$.

This example proves that in certain configurations, the drag can be diminished by increasing the value of the friction coefficient in specific regions of the boundary of the solid.

Example 5.3 (Optimization of the drag with respect to β.) In order to approach realistic situations, we fix a minimal value $\beta_{min} > 0$ of the friction coefficient, and consider the following minimization problem:

$$\min \left\{ T(\beta, \mathbf{u}) \mid \beta \geqslant \beta_{min} \right\}. \tag{19}$$

To deal with this constrained optimization problem, we use a projective gradient method. The computation of the gradient of the drag with respect to β relies on the following result, which is proved in [1]. Let ν be large enough such that problem (1)–(3), (17)–(18) has a unique weak solution, denoted $(\mathbf{u}_\beta, p_\beta)$ and $\mathbf{u}_\infty \in \mathbb{R}$. The unique drag $T(\beta, \mathbf{u}_\beta)$ is simply denoted $T(\beta)$. We introduce the following subset of $L^2(\partial S)$:

$$\mathcal{O} = \left\{ \beta \in L^2(\partial S) \mid \beta > 0 \text{ a.e. on } \partial S \right\}.$$

Proposition 5.4 *The mapping*

$$\beta \in \mathcal{O} \to T(\beta) \in \mathbb{R}$$

is differentiable in $L^2(\partial S)$, and its gradient is given by

$$\nabla T(\beta) = \left[(\mathbf{u}_\beta + \psi) \cdot \mathbf{u}_\beta \right]_{|\partial S}, \tag{20}$$

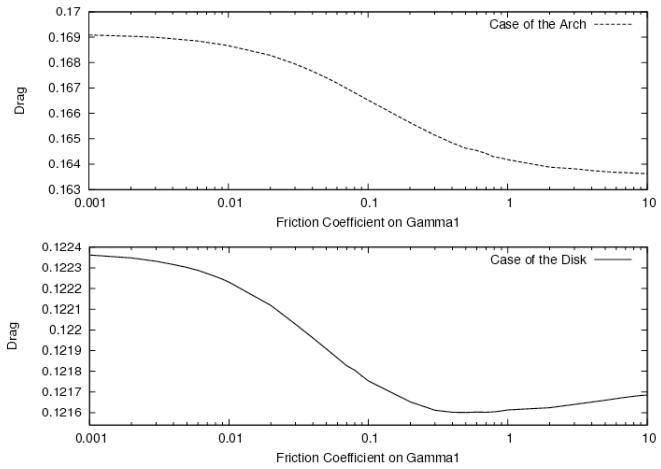

Figure 4: Drag versus constant values of β on $\partial S_2 \setminus \Gamma_1$ (resp. on $\partial S_1 \setminus \Gamma_1$) with $\beta = 10$ on Γ_1.

where $\psi \in H^1(\Omega \setminus S, \mathbb{R}^2)$ *is the unique solution to the adjoint system*

$$\begin{cases} -\text{div } (\sigma(\psi, p)) + (\nabla \mathbf{u})^T \psi - (\mathbf{u} \cdot \nabla)\psi = & 2(\mathbf{u} \cdot \nabla)\mathbf{u} \text{ in } \Omega \setminus S, \\ \text{div } \psi = & 0 \text{ in } \Omega \setminus S, \\ \psi = & 0 \text{ on } \partial\Omega, \\ \psi \cdot \mathbf{n} = & 0 \text{ on } \partial\mathcal{S}, \\ [2\nu \mathbf{D}(\psi)\mathbf{n}]_{tan} + \beta\psi = & 0 \text{ on } \partial\mathcal{S}. \end{cases} \tag{21}$$

In this example, we deal with the arch S_2. We fix a constant value of the step $h = 10000$ in the gradient descent and a stopping criterion $\epsilon = 10^{-5}$ for the L^2 norm of the projected gradient on ∂S_2. The initial friction coefficient has a constant value $\beta \equiv 5$, and we set the minimal value of the friction $\beta_{min} = 1$.

In Table 1, we give the value of the drag and the L^2 norm of the projected gradient at the first iterations, at convergence of the algorithm (iteration 27) and at several intermediate iterations. The minimal value of the drag is 3.14% inferior to the initial value with $\beta \equiv 5$. Furthermore, in comparison, the value of the drag for $\beta \equiv 1$ (which we have computed to plot Figure 3) is equal to 0.159271. This confirms that the uniform distribution $\beta \equiv 0.5$ is not optimal for the minimization problem (19).

In Figure 5, we have plotted the friction coefficient on each side of the boundary of the arch, namely, on $\Gamma_2 \cup \Gamma_3 \cup \Gamma_4$ and on Γ_1, with respect to the ordinate of the points on the boundary, after 1 step of the descent and at convergence of the algorithm. At convergence, we can observe that the friction has globally increased in the prominent parts of the obstacle, namely, the semicircles Γ_2 and Γ_4, to reach 3 or 4 times its initial value, except for a small vicinity of the junction points with Γ_1 where the friction has decreased and the constraint $\beta \geqslant \beta_{min}$ is saturated. On the contrary, the value of the friction on the hollow part of the boundary Γ_3 has not been modified during the process. On the other side of the arch, there is a significant increase of the friction on a large vicinity of the extremal points of Γ_1, except for a very small region near these points where the friction decreases to reach the minimal

Iteration	Drag	L^2 norm
0	0.163521	33.0758
1	0.160299	10.4981
2	0.158421	9.6474
3	0.158398	5.33867
4	0.158383	4.17234

Table 1: Drag and L^2 norm of the projected gradient in the gradient descent.

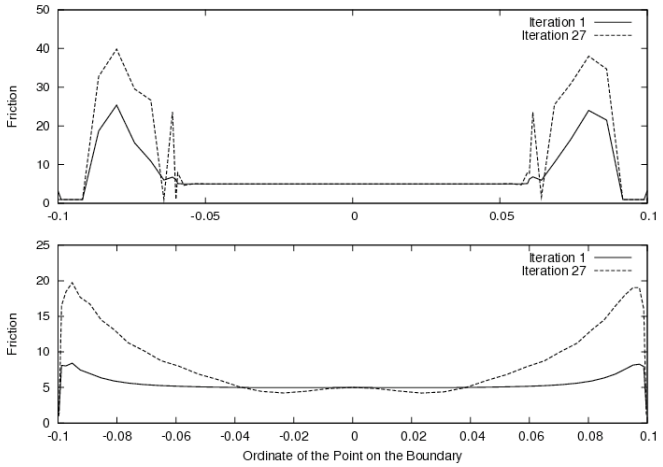

Figure 5: Friction coefficient on $\Gamma_2 \cup \Gamma_3 \cup \Gamma_4$ (top) and Γ_1 (bottom), with respect to the ordinate of the point on the boundary, after 1 step and 4 steps of the gradient descent.

value β_{min} and connect with the value on the other side of the junction points. The friction in a middle region around the axis $y = 0$ remains close to the initial value $\beta = 5$.

This example confirms that using the rugosity in order to increase the friction coefficient on certain specific parts on the boundary of a solid, may contribute to diminish the drag.

References

[1] M. Bonnivard, *Titre*, PhD Thesis, Université de Savoie, 2010.

[2] D. Bucur and G. Buttazzo, *Variational methods in shape optimization problems*, Progress in Nonlinear Differential Equations and their Applications, 65, Birkhäuser Boston Inc., Boston, MA, 2005.

[3] D. Bucur, E. Feireisl, and Š. Nečasová, *Boundary behavior of viscous fluids: Influence of wall roughness and friction-driven boundary conditions*, Arch. Ration. Mech. Anal., 197 (2010), pp. 117–138.

[4] D. Bucur and J.-P. Zolésio, *N-dimensional shape optimization under capacitary constraint*, J. Differential Equations, 123 (1995), pp. 504–522.

[5] G. Dal Maso, *An introduction to Γ-convergence*, Progress in Nonlinear Differential Equations and their Applications, 8, Birkhäuser Boston Inc., Boston, MA, 1993.

[6] Z. Gao, Y. Ma, and H. Zhuang, *Drag minimization for Navier-Stokes flow*, Numer. Methods Partial Differential Equations, 25 (2009), pp. 1149–1166.

[7] L. I. Hedberg, *Spectral synthesis in Sobolev spaces, and uniqueness of solutions of the Dirichlet problem*, Acta Math., 147 (1981), pp. 237–264.

[8] A. Henrot and M. Pierre, *Variation et Optimisation de Formes*, Mathématiques et Applications, Springer-Verlag, Berlin, 2005.

[9] W. Jäger and A. Mikelić, *Couette flows over a rough boundary and drag reduction*, Comm. Math. Phys., 232 (2003), pp. 429–455.

[10] B. Mohammadi and O. Pironneau, *Applied shape optimization for fluids*, Numerical Mathematics and Scientific Computation, The Clarendon Press Oxford University Press, New York, 2001. Oxford Science Publications.

[11] B. Mohammadi and O. Pironneau, *Applied shape optimization for fluids*, Numerical Mathematics and Scientific Computation, Oxford University Press, Oxford, second ed., 2010.

[12] P. I. Plotnikov, E. V. Ruban, and J. Sokolowski, *Shape differentiability of drag functional for compressible Navier-Stokes equations*, in Optimal control of coupled systems of partial differential equations, vol. 158 of Internat. Ser. Numer. Math., Birkhäuser Verlag, Basel, 2009, pp. 205–219.

[13] J. Simon, *Domain variation for drag in Stokes flow*, in Control theory of distributed parameter systems and applications (Shanghai, 1990), vol. 159 of Lecture Notes in Control and Inform. Sci., Springer, Berlin, 1991, pp. 28–42.

[14] S. Vogel, *Life in moving of fluids; the physical biology of flow*, Numerical Mathematics and Scientific Computation, Princeton University Press, 1994. Princeton, N.J.

[15] W. P. Ziemer, *Weakly differentiable functions*, vol. 120 of Graduate Texts in Mathematics, Springer-Verlag, New York, 1989. Sobolev spaces and functions of bounded variation.